Mon. Not. R. Astron. Soc. **000**, 1–6 (2014) Printed 12 August 2014 (MN LATEX style file v2.2)

The role of the reflection fraction in constraining black hole spin

T. Dauser[1⋆], J. García[2], M.L. Parker[3], A.C. Fabian[3] and J. Wilms[1]
[1] *Dr. Karl Remeis-Observatory and Erlangen Centre for Astroparticle Physics, Sternwartstr. 7, 96049 Bamberg, Germany*
[2] *Harvard-Smithsonian Center for Astrophysics, 60 Garden Street, Cambridge, MA 02138, USA*
[3] *Institute of Astronomy, Madingley Road, Cambridge CB3 0HA*

arXiv:1408.2347v1 [astro-ph.HE] 11 Aug 2014

12 August 2014

ABSTRACT
In many active galaxies, the X-ray reflection features from the innermost regions of the accretion disc are relativistically distorted. This distortion allows us to measure parameters of the black hole such as its spin. The ratio in flux between the direct and the reflected radiation, the so-called reflection fraction, is determined directly from the geometry and location of primary source of radiation. We calculate the reflection fraction in the lamp post geometry in order to determine its maximal possible value for a given value of black hole spin. We show that high reflection fractions in excess of 2 are only possible for rapidly rotating black holes, suggesting that the high spin sources produce the strongest relativistic reflection features. Using simulations we show that taking this constraint into account does significantly improve the determination of the spin values. We make software routines for the most popular X-ray data analysis packages available that incorporate these additional constraints.

Key words: accretion, accretion discs, black hole physics, galaxies: active, galaxies: active

1 INTRODUCTION

Reflection of X-rays off the innermost parts of the accretion disc is highly affected by general relativistic effects, leading to strong broadening of the reflection features (see, e.g., Fabian et al. 1989; Laor 1991; Reynolds & Nowak 2003; Miller 2007; Dauser et al. 2010). Such broadened reflection features are found in a large number of active galactic nuclei (AGN), such as, e.g., MCG−6-30-15 (Tanaka et al. 1995; Wilms et al. 2001; Fabian & Vaughan 2003; Marinucci et al. 2014), 1H0707−495 (Fabian et al. 2009; Dauser et al. 2012), or NGC 1365, (Risaliti et al. 2013), Galactic Black Holes, such as Cyg X-1 (Fabian et al. 1989; Duro et al. 2011; Tomsick et al. 2014), GRS 1915+10 (Miller et al. 2013b), or GX 339−4 (Miller et al. 2008; Reis et al. 2008), and neutron stars (e.g., Serpens X-1; Miller et al. 2013a). Although measurements of high-frequency Fe-K reverberation strongly support the reflection origin of these broadened features (see, e.g., Kara et al. 2013; Uttley et al. 2014), the spectrum alone can generally be also described by partial covering an ionized absorber (see, e.g., Miller, Turner & Reeves 2008, 2009). However, this interpretation will not be pursued any further in this letter, as the presented results are only applicable if a reflection origin of the broadened spectrum is preferred.

The origin of the primary X-ray radiation causing this reflection is still under debate. Although a standard corona of hot electrons around the inner parts of the accretion disc is able to explain the observed power law spectrum (e.g., Haardt 1993; Dove et al. 1997; Belmont, Malzac & Marcowith 2008), it generally fails to explain the very steep emissivities deduced from the Fe Kα profiles for the inner parts of the accretion disc (see, e.g., Wilms et al. 2001; Fabian et al. 2004; Brenneman & Reynolds 2006; Ponti et al. 2010; Brenneman et al. 2011; Gallo et al. 2011; Dauser et al. 2012; Risaliti et al. 2013). A primary source on the rotational axis above the black hole, however, is able yield these steeper emissivities (Matt, Perola & Piro 1991; Martocchia & Matt 1996). If this source is associated with the base of a jet (Markoff & Nowak 2004), besides the steep emissivity, this so called "lamp post" geometry is also able to explain the spectral connection of the X-ray and radio radiation (e.g., Markoff, Nowak & Wilms 2005; Maitra et al. 2009). See Dauser et al. (2013) for a more detailed discussion.

In absence of opaque material that obstructs the central emission region, an observer will always see the sum of direct radiation from the primary source of X-rays and the reflected component. In the classical limit, the ratio of the flux in the reflected component to that from the primary source is the same. This ratio, referred to as the *Reflection Fraction*, R, can be significantly enhanced when the source height is reduced due to the light bending effects near the black hole (Miniutti & Fabian 2004). In addition, the dependence of the location of the inner edge of the accretion disc from the black hole's spin, a, also modifies the area of the reflector and thus the amount of reflection. The reflection fraction therefore encodes important information about the geometry of the reflector. While the spin is routinely determined through spectral fitting of reflection models, most models neglected the dependence of R on a, leaving R as a free parameter in previous studies.[1] The RELX-

⋆ E-mail: thomas.dauser@sternwarte.uni-erlangen.de

[1] Note that although the `pexrav` model (Magdziarz & Zdziarski 1995) in-

© 2014 RAS

ILL model presented by García et al. (2014) is the first model which allows us to directly fit the reflection fraction of a relativistically smeared reflection spectrum.

If the geometry and location of the primary source are known, then R can be easily calculated, given the angular dependence of the emission pattern. In practice, however, except for a rough compactness criterion (source inside $< 10\,r_{\rm g}$, Fabian et al. 2014), the exact geometry of the illumination has not been unambiguously determined for any source yet. In this *Letter* we present calculations of the reflection fraction R predicted in a lamp post geometry for different configurations of the source height and black hole spin. A maximum value of R is then determined for a given value of spin, which can be used to exclude unphysical solutions of low spin and large reflection fractions. We demonstrate that this constraint has a dramatic effect in improving the constraints on the spin determinations, which in turn provides insights on the nature of the geometry of the illumination source.

2 THE MAXIMUM REFLECTION FRACTION

2.1 Determination of the Reflection Fraction

The reflection fraction is defined as the ratio between the reflected and direct radiation,

$$R := \frac{f_{\rm AD}}{f_{\rm INF}} = \frac{\cos\delta_{\rm in} - \cos\delta_{\rm out}}{1 + \cos\delta_{\rm out}} \qquad (1)$$

where the fraction has been determined for the case of the lamp post geometry, assuming a stationary, isotropic primary source. Here, $f_{\rm AD}$ and $f_{\rm INF}$ denote the fraction of the photons hitting the accretion disc or escaping to infinity, respectively, and $\delta_{\rm in}$ and $\delta_{\rm out}$ are the angles under which photons hit the inner and outer edge of the disc, respectively (Fukumura & Kazanas 2007). In the non-relativistic case and an infinitely extended accretion disc $R = 1$, i.e., half of the photons reach infinity while the other half are reflected from the disc. This definition of R is identical to the *covering fraction* used in most reflection models such as `pexrav` (Magdziarz & Zdziarski 1995), where it is used to describe distant neutral reflection. However, as relativistic reflection originates from an ionized disc very close to the black holes, the values of R obtained with `pexrav` cannot be compared with our results presented in the following. Also note that the reflection fraction in this letter does not include any contribution from this distant reflection by definition. In the case of the lamp post model, as already noticed previously (Miniutti & Fabian 2004), when the source height decreases, strong gravitational beaming reduces the number of photons that reach infinity while $f_{\rm AD}$ increases, thus enhancing the reflection features (see Fig. 1). As a consequence of these effects, the maximum possible reflection fraction depends on the spin.

For the purpose of finding an upper limit to R, we use the simplified lamp post geometry, which assumes a point-like, isotropic source on the rotational axis of the black hole (Martocchia & Matt 1996). First calculations of the reflection fraction for a lamp-post like geometry were performed by Miniutti et al. (2003) for a ring-like primary source around an extreme Kerr black hole, while Fukumura & Kazanas (2007) analysed a point-like lamp post for different spin configurations of the black hole. We determine the reflection spectrum using the code presented by Dauser et al. (2013),

cludes R as a fitting parameter, it is only suitable to describe distant neutral reflection.

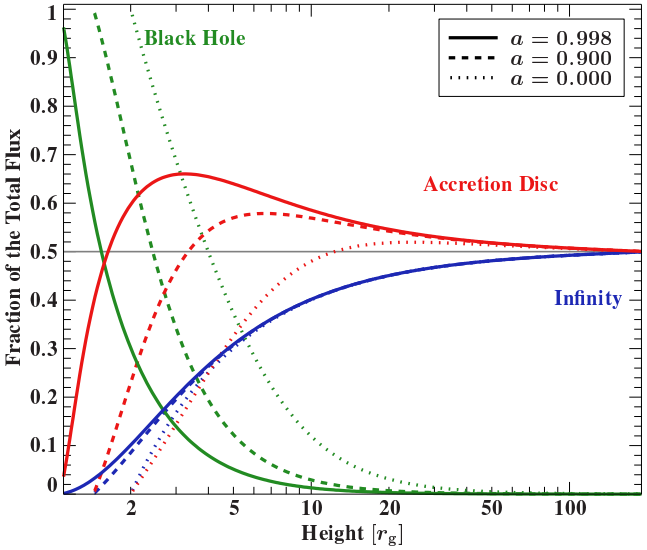

Figure 1. Fraction of the total flux ending up in the black hole (green), hitting the accretion disc (red), or leaving the system (blue). The calculation assumes a non-moving, isotropic radiating source on the axis of symmetry of the accretion flow, fractions are shown as a function of height of the primary source, given in units of the gravitational radius, $r_{\rm g} = GM/c^2$.

which is based on algorithms provided by Speith, Riffert & Ruder (1995). The maximum reflection fraction is obtained for the case of the accretion disc extending from the innermost stable circular orbit (ISCO) out to infinity, for the cases covered by Fukumura & Kazanas (2007), our results agree with the earlier calculations.

2.2 The Maximum Reflection Fraction

Fig. 2 shows how the reflection fraction varies with the height of the source above the black hole and with black hole spin. Except for the case of extreme spin, if the source is close to the black hole the severe beaming of photons combined with the larger inner disc radius reduces the flux that reaches the accretion disc and the reflection fraction is small. On the other hand, if the primary source is too far away from the black hole, $R \gtrsim 10 r_{\rm g}$, relativistic effects diminish in importance and R converges towards its non-relativistic limit. There is therefore a spin-dependent maximum reflection fraction, $R_{\rm max}$. As shown in the left panel of Fig. 3, for low values of a, this maximum is only slightly higher than its non-relativistic value, while for higher spin $R_{\rm max}$ increases steeply.

A different way to illustrate the behaviour is shown in the right panel of Fig. 3, which shows that a very similar relation is obtained when fixing the spin, but allowing the inner edge of the accretion disc to vary. Again, for a growing inner radius the maximal reflection fraction quickly declines. This similarity between changing the inner radius and changing the spin of the black is not surprising. As shown, e.g., by Dauser et al. (2010), the main effect of the spin on the observed spectrum is to define the location of the ISCO.

Fig. 4 shows how the height of the point above the black hole from which the maximum reflection is reached changes with spin. Surprisingly, this location follows an almost linear trend which is is well fitted by the empirical relationship

$$h_{R_{\rm max}}(a) = (1.89a^2 - 10.86a + 10.07)\left(1 + \frac{9.41\times10^{-4}}{\log(a)}\right) \qquad (2)$$

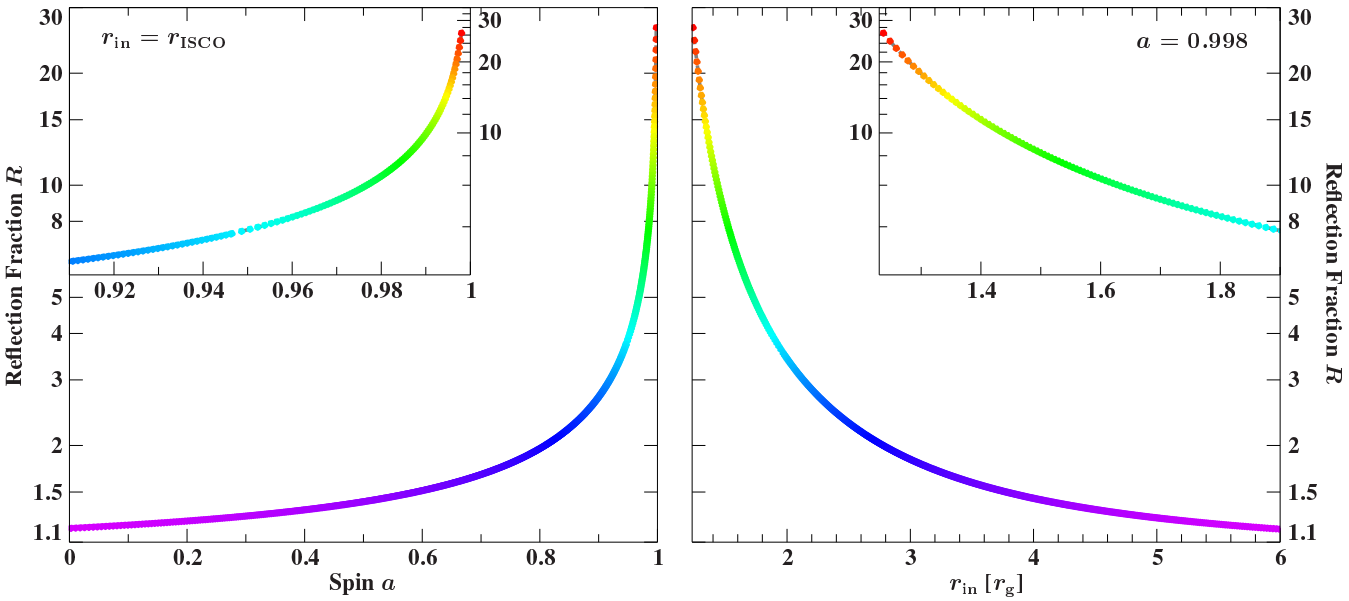

Figure 3. Left: maximum possible reflection fraction $R_{\rm max}$ as a function of spin, assuming that the accretion disc extends down to the ISCO. Right: maximum possible reflection fraction for a maximally spinning black hole ($a = 0.998$) as a function of the location of the inner edge of the accretion disc $r_{\rm in}$. The colour scale of the points is identical to Fig. 4.

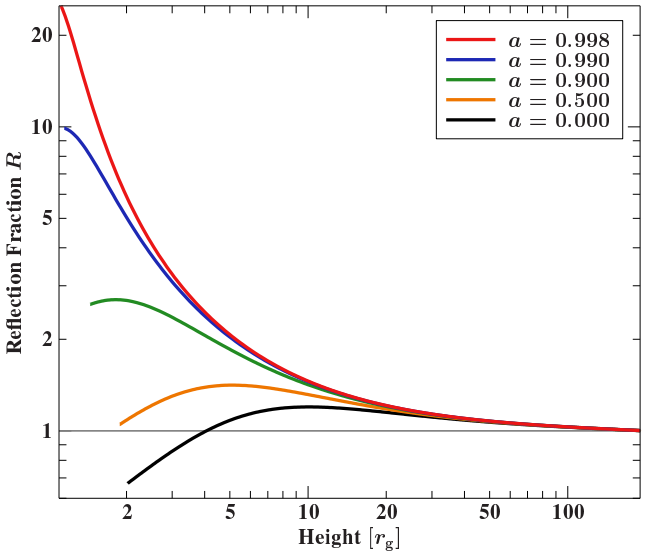

Figure 2. Reflection fraction for a point-like lamp post source.

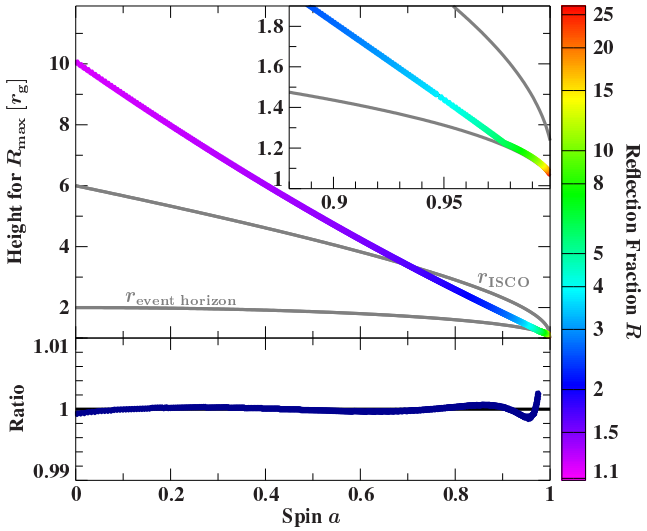

Figure 4. The height at which the maximum reflection fraction $R_{\rm max}$ is reached as a function of a follows approximately a linear trend. The lower panel shows the ratio between the fit (Eq. 2) and the simulated data.

For $a < 0.975$, Eq. 2 has a precision $< 0.1\%$. Above this value of spin, the irradiating source is located directly on the event horizon of the black hole and thus $h(R_{\rm max}) = 1 + \sqrt{1 - a^2}$.

We note that a point-like primary source as assumed above is only a first-order description of the real physical system, which is likely extended in size. However, only compact sources that are close to the black hole will lead to a strong broadening of the Fe Kα lines (Dauser et al. 2013; Fabian et al. 2014), which is essential for reliable spin estimates (e.g., 1H0707−495 or NGC 1365). Furthermore, since an extended source can be treated as the superposition of point sources (e.g., Dauser et al. 2010, 2013; Wilkins & Fabian 2012), it is easy to see that the broadening of the reflection spectrum will be dominated by the emission from the point where the flux intercepted by the disc is at a maximum (Fig. 1, see also Eq. 2 and Fig. 4 below). On the other hand, if the primary source is off-axis and point like X-rays will be less focused towards the disc, and therefore the maximum reflection fraction will be less than or equal to that from a source that is on axis. It is only in the special cases of irradiating sources which are extended parallel to the disc surface (e.g., the "disc like" primary source inferred by Wilkins & Fabian 2011) or in the case of an inflowing corona which is beamed towards the disc that slightly higher reflection fractions than the ones presented in the left panel of Fig. 3 could be reached.

In some extreme cases, however, the reflection fraction measured by an observer might be different from the theoretical one calculated (Eq. 1). While the latter is defined as the total reflected flux, the observer only sees the system under a certain inclination

angle and in the measurement of R also needs to disentangle inclination effects. This is especially difficult at high inclinations, where strong beaming of the radiation along the equatorial plane (see, e.g., Sun & Malkan 1989; Miniutti & Fabian 2004) and limb brightening effects are expected (García et al. 2014). Combining these effects in a Monte Carlo simulation, Suebsuwong et al. (2006) have shown that larger values R will only be measured for very high inclination angles (i.e., $\theta \gtrsim 85°$). Clearly, these inclinations are too extreme for observing the emission from the inner regions of the accretion discs in AGN, as the reflection features would be smeared out and the SMBH is likely to be unobservable in presence of a torus.

2.3 Constraints for Spin Measurements

The fact that there is a maximum reflection fraction can be used to constrain the parameter space when modelling observational data by excluding unphysical solutions for the spin parameter. For example, for low spins, $a < 0.5$, $R_{\rm max} < 1.5$. Any solution requiring a significantly higher reflection fraction at the same time with requiring a low spin poses difficulties for interpreting the data. In many cases a different combination of parameters with a high value of the spin might be a more realistic description of the system. The reflection fraction also puts constraints on truncated discs: An inner radius larger than a few gravitational radii will at maximum lead to values slightly larger than $R = 1$ (Fig. 3, right panel). Fits with truncated discs are therefore incompatible with larger reflection fractions.

In order to illustrate the large potential of the presented constraint on spin measurements, we simulate a typical observation of a low state AGN with *XMM-Newton*. Compared to broad-band measurements which include the reflection hump in the 20–50 keV band and provide a stronger constraint on R, measurements in the soft X-rays are especially prone to systematic errors due to foreground emission and absorption processes. These systematic errors tend to affect the continuum in the iron band, and therefore the major spectral component sensitive to a. Additional constraints such as that for $R_{\rm max}$ are therefore especially valuable for modelling soft X-ray data.

Fig. 5 shows χ^2-contours obtained from fitting the continuum model to the simulated spectra, with all the parameters free to vary, both with and without the $R_{\rm max}$ constraint. It is immediately evident that this constraint yields not only a better spin estimate, but also that the unconstrained fit would yield an incorrect value of the spin parameter ($a \sim 0.55$) in the case where $R = 2$. Taking the maximum reflection fraction into account therefore avoids possible unphysical solutions, while also reducing the uncertainties on the spin parameter directly. Note that while a more complicated spectrum (e.g., including distant reflection) generally leads to weaker constraints on the spin, the improvement of this constraint when enforcing $R_{\rm max}$ is still significant.

3 SUMMARY AND CONCLUSIONS

We presented a determination of the reflection fraction in the lamp post geometry. Our aim was to derive a relation for the maximum possible reflection fraction depending on the spin of the black hole. We could show that this relation approaches the non-relativistic value of $R = 1$ quickly and therefore strongly limits the effective parameter space of R for lower values of spin. A very similar behaviour is found for constant spin and a growing inner radius of the accretion disc. Simulating observations and applying the additional constraint that R is at the maximum value possible for a given spin revealed that in this way unphysical solutions can be excluded and better constraints on a could be obtained.

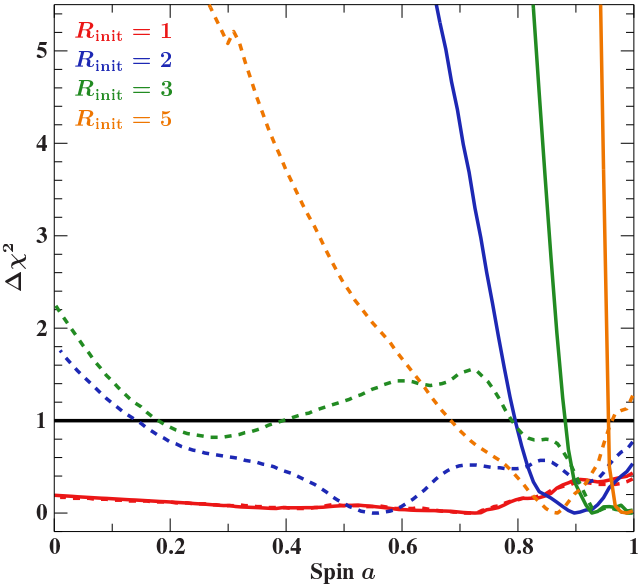

Figure 5. Shape of the χ^2-valley for a typical 100 ks long AGN observation with the EPIC-pn detector on *XMM-Newton*. Shown is the difference of χ^2 with respect to the best-fitting value, with $\Delta\chi^2 = 1$ corresponding to the 1σ confidence interval (Lampton, Margon & Bowyer 1976). Solid lines indicate fits taking the reflection fraction constraint into account, dotted lines are fits where the constraint is ignored. The underlying continuum is based on the low state of 1H0707−495, a simple absorbed powerlaw plus reflection model, TBABS×RELXILL, with a 0.3–10 keV flux of $10^{-12}\,{\rm erg\,s^{-1}\,cm^{-2}}$, a photon index $\Gamma = 2$, $N_{\rm H} = 10^{20}\,{\rm cm^{-2}}$, an emissivity index to 3, $a = 0.97$, an inclination of 30°, and an ionization parameter $\xi = 100\,{\rm erg\,cm\,s^{-1}}$ with an iron abundance that is three times solar. In order to see how well the spin is constrained, the same model is fit to the simulated data for different values of spin a. All fit parameters except for a are allowed to vary in the fits.

To allow observers to take into account these additional constraints, we have made available a new implementation of the RELXILL model[2] (Dauser et al. 2013; García et al. 2014) in which the reflection fraction can either be fixed to the theoretical prediction of the lamp post model or fitted independently.

Measurements of the reflection fractions are usually scarce and inconsistent. However, some spectral surveys of local AGN have made estimates of R by fitting the reflection signatures (e.g. Nandra et al. 2007; Brenneman & Reynolds 2009; Patrick et al. 2012). Recently, Walton et al. (2013) presented a study of 25 "bare AGN" (with no evidence for warm absorbers or any other intervening material), providing perhaps the first consistent estimate for the strength of the ionized reflection (rather than the distant, neutral reflection) in a large sample of AGN. Although their values of R are approximate, they find a strong preference for reflection fractions near unity, which agrees well with our theoretical predictions. There is only one case, 1H0707−495, for which the reflection fraction is extremely high ($R = 275$) despite its extreme spin ($a > 0.994$), but the source was in a particularly low state

[2] The RELXILL model can be downloaded at `http://www.sternwarte.uni-erlangen.de/research/relxill/`.

when the direct power law continuum is difficult to constrain. It is particularly interesting to note that our simulation for $R = 2$ (Fig. 5) resembles in many cases the χ^2 confidence contours shown by Walton et al. (2013, their fig. 2), in particular the tendency of finding two different solutions for the spin. Good examples are Mrk 841, 1H0323+342, UGC 6728, Mrk 359, and Mrk 1018. This behaviour can be interpreted as a consequence of certain degeneracy between the amount of reflection and the spin. This degeneracy can be removed by implementing the constraint on the maximum value of R presented in this letter. Note that in certain cases measuring the reflection component of the spectrum can be challenging, as overlying absorption and emission processes complicate the flux determination of the reflected radiation. Therefore the best measure is to use the flux of the featureless Compton hump (roughly between 20 and 40 keV). Due to the negligible photoelectric absorption above 15keV (see, e.g., García et al. 2013), the elemental abundances have only a negligible influence on R. However, note that distant reflection might complicate this determination.

A second observational consequence of our results is the recently growing number of spin measurements which suggest that a large fraction of the observed black holes are rapidly spinning (see, e.g., Reynolds 2013). In principle this distribution would allow us to draw conclusions about the evolution of black hole spin (e.g., Volonteri et al. 2005; King, Pringle & Hofmann 2008). However, as can be seen in the left panel of Fig. 3, for not extremely spinning black holes $R_{\rm max}$ is already close to 1. Sources with lower spin are therefore expected to show a much weaker reflection component, which, depending on the quality of the data, is generally harder to be detected. Moreover, a low spin or a larger source height means less pronounced relativistic reflection (e.g., Dauser et al. 2013). Combined with the effect that these configurations also lead to lower reflection fractions (see also Fig. 2), will make the broad emission features from such objects much harder to detect than from rapidly spinning black holes. A stronger bias towards highly rotating black holes is therefore expected. Also note that using standard accretion disc theory, any flux limited sample is already biased towards detecting high spin sources, due to a larger radiative efficiency for increasing spin (see Brenneman et al. 2011).

Acknowledgements. TD acknowledges support by a fellowship from the Elitenetzwerk Bayern, and by the Deutsches Zentrum für Luft- und Raumfahrt under contract number 50 OR 1113. JG acknowledges the support of NASA grant NNX11AD08G. We thank John E. Davis for the development of the SLXFIG module used to prepare the figures in this letter. This research has made use of ISIS functions provided by ECAP/Remeis observatory and MIT (http://www.sternwarte.uni-erlangen.de/isis/).

REFERENCES

Belmont R., Malzac J., Marcowith A., 2008, A&A, 491, 617
Brenneman L. W., Reynolds C. S., 2006, ApJ, 652, 1028
Brenneman L. W., Reynolds C. S., 2009, ApJ, 702, 1367
Brenneman L. W. et al., 2011, ApJ, 736, 103
Dauser T., García J., Wilms J., Böck M., Brenneman L. W., Falanga M., Fukumura K., Reynolds C. S., 2013, MNRAS, 687
Dauser T. et al., 2012, MNRAS, 422, 1914
Dauser T., Wilms J., Reynolds C. S., Brenneman L. W., 2010, MNRAS, 409, 1534
Dove J. B., Wilms J., Maisack M., Begelman M. C., 1997, ApJ, 487, 759
Duro R. et al., 2011, A&A, 533, L3
Fabian A. C., Miniutti G., Gallo L., Boller T., Tanaka Y., Vaughan S., Ross R. R., 2004, MNRAS, 353, 1071
Fabian A. C., Parker M. L., Wilkins D. R., Miller J. M., Kara E., Reynolds C. S., Dauser T., 2014, MNRAS, 439, 2307
Fabian A. C., Rees M. J., Stella L., White N. E., 1989, MNRAS, 238, 729
Fabian A. C., Vaughan S., 2003, MNRAS, 340, L28
Fabian A. C. et al., 2009, Nat, 459, 540
Fukumura K., Kazanas D., 2007, ApJ, 664, 14
Gallo L. C., Miniutti G., Miller J. M., Brenneman L. W., Fabian A. C., Guainazzi M., Reynolds C. S., 2011, MNRAS, 411, 607
García J. et al., 2014, ApJ, 782, 76
García J., Dauser T., Reynolds C. S., Kallman T. R., McClintock J. E., Wilms J., Eikmann W., 2013, ApJ, 768, 146
Haardt F., 1993, ApJ, 413, 680
Kara E., Fabian A. C., Cackett E. M., Uttley P., Wilkins D. R., Zoghbi A., 2013, MNRAS, 434, 1129
King A. R., Pringle J. E., Hofmann J. A., 2008, MNRAS, 385, 1621
Lampton M., Margon B., Bowyer S., 1976, ApJ, 208, 177
Laor A., 1991, ApJ, 376, 90
Magdziarz P., Zdziarski A. A., 1995, MNRAS, 273, 837
Maitra D., Markoff S., Brocksopp C., Noble M., Nowak M., Wilms J., 2009, MNRAS, 398, 1638
Marinucci A. et al., 2014, ApJ, in press (arXiv:1404.3561)
Markoff S., Nowak M. A., 2004, ApJ, 609, 972
Markoff S., Nowak M. A., Wilms J., 2005, ApJ, 635, 1203
Martocchia A., Matt G., 1996, MNRAS, 282, L53
Matt G., Perola G. C., Piro L., 1991, A&A, 247, 25
Miller J. M., 2007, ARA&A, 45, 441
Miller J. M. et al., 2013a, Astrophys. J., Lett., 779, L2
Miller J. M. et al., 2013b, Astrophys. J., Lett., 775, L45
Miller J. M. et al., 2008, ApJ, 679, L113
Miller L., Turner T. J., Reeves J. N., 2008, A&A, 483, 437
Miller L., Turner T. J., Reeves J. N., 2009, MNRAS, 399, L69
Miniutti G., Fabian A. C., 2004, MNRAS, 349, 1435
Miniutti G., Fabian A. C., Goyder R., Lasenby A. N., 2003, MNRAS, 344, L22
Nandra K., O'Neill P. M., George I. M., Reeves J. N., 2007, MNRAS, 382, 194
Patrick A. R., Reeves J. N., Porquet D., Markowitz A. G., Braito V., Lobban A. P., 2012, MNRAS, 426, 2522
Ponti G. et al., 2010, MNRAS, 406, 2591
Reis R. C., Fabian A. C., Ross R. R., Miniutti G., Miller J. M., Reynolds C., 2008, MNRAS, 387, 1489
Reynolds C. S., 2013, Classical and Quantum Gravity, 30, 244004
Reynolds C. S., Nowak M. A., 2003, Phys. Rep., 377, 389
Risaliti G. et al., 2013, Nat, 494, 449
Speith R., Riffert H., Ruder H., 1995, Comp. Phys. Commun., 88, 109
Suebsuwong T., Malzac J., Jourdain E., Marcowith A., 2006, A&A, 453, 773
Sun W.-H., Malkan M. A., 1989, ApJ, 346, 68
Tanaka Y. et al., 1995, Nat, 375, 659
Tomsick J. A. et al., 2014, ApJ, 780, 78
Uttley P., Cackett E. M., Fabian A. C., Kara E., Wilkins D. R., 2014, accepted (arXiv:1405.6575)
Volonteri M., Madau P., Quataert E., Rees M. J., 2005, ApJ, 620, 69
Walton D. J., Nardini E., Fabian A. C., Gallo L. C., Reis R. C., 2013, MNRAS, 428, 2901
Wilkins D. R., Fabian A. C., 2011, MNRAS, 414, 1269

Wilkins D. R., Fabian A. C., 2012, MNRAS, 424, 1284
Wilms J., Reynolds C. S., Begelman M. C., Reeves J., Molendi S., Staubert R., Kendziorra E., 2001, MNRAS, 328, L27